Electrochemical Characterization of Low and Non-Platinum Catalysts for Fuel Cell Applications in Gas Diffusion Electrodes Setup

Talal Ashraf
talal.ashraf@tecnico.ulisboa.pt
Instituto Superior Técnico, Universidade de Lisboa Portugal
September 2020

Abstract*—Fuel cell electrocatalysts are constrained by various factors, most importantly, the precious catalysts leading to the development and exploration of the novel, cheap and highly effective and stable electrocatalyst. In this work, novel optimised gas diffusion electrode half-cell benchmarking tool is utilised for determining the sluggish kinetics of ORR electrocatalyst that aims to bridge the gap between two conventional and fundamental and applied electroanalytical devices as RDE and MEA. To analyse the versatility of GDE method, various catalysts were evaluated to optimise the catalyst layer such as commercial Pt/C catalyst, advanced Pt/HGS catalyst and non PGM Fe-N-C catalyst. The Pt/C proved to be high performing catalyst with ECSA of 66.59 m^2/g_{pt} approaching to limiting current density of 2 A/cm^2 at 0.63 V_{RHE} in 1.0 M $HClO_4$. As compared to $HClO_4$, the Pt/C suffered from severe degradation in 1.0 M H_2SO_4 facing mass transport limitation. The addition of membrane to commercial Pt/C in both electrolytes to mimic the conditions of PEMFC gave a comparable activity with less degradation. However, the Pt/C approached to extreme mass transport limitation in synthetic air due to low concentration of O_2 and contamination in the air. The performance of Pt/C in alkaline was superior by achieving limiting current density of 2 A/cm^2 at 0.8 V_{RHE}, which was highest in comparison to literature and it is believed to be overestimated due to huge difference for forward and backward scans. Stress cycling of confined Pt nanoparticles supported on highly graphitised Pt/HGS improved the catalyst activity. After subjecting to 10,000 and 30,000 cycles, the ORR activity enhanced up to 50 mV and thus, the catalyst layer was optimised accordingly. AEMFC conditions were also be mimicked in GDE cell with non PGM catalyst Fe-N-C which was investigated in 1.0 M KOH for the stability, ionomer activation and reproducibility. The catalyst layer was optimised with high ion exchange ionomers, and it has been found that the catalyst activity can be enhanced to approximately 80-100 mV by several breaking and time-based(max 48 hours) ionomer activation procedures. The Fe-N-C proved to be stable during ORR in O_2 but faced severe degradation in O_2 backed degradation cycling. Thus, GDE is proved to be a very effective method for quicker, reliable optimisation of electrocatalyst performance but with several challenges which are discussed in this work and it can be used to optimise the catalyst layer properties with minimum efforts. More comprehensive analysis can be addressed by merging different characterisation mechanism and metal ions dissolution quantification techniques that will enable this method to be upgraded for fuel cell electrocatalyst research and development sector.

***Index Terms*—Oxygen reduction reaction; Non precious metal group catalyst; Platinum confinement; Gas diffusion electrode; AEMFC; PEMFC.**

I. Introduction

GLOBAL warming with increasing greenhouse gases concentration caused by anthropogenic activities is imposing drastic changes in eco and biosphere. Due to high energy demand, the CO_2 emissions surged up to 1.7% with 33.1 Gt CO_2 in 2018. According to Environmental Indicator Report by European Economic Area in 2018, the objective of green and low carbon economy from greenhouse gases reduction from transport is unlikely to be achieved by 7^{th} Environmental Action Plan implementation (2014-2020). The transportation section contributes as a major role in greenhouse gases emission, in 2017 around 27% of total EU emissions come from transportation section, making it the second biggest pollutant emitter after energy production sector[1].

The infrastructure for fuel cell vehicles (FCV) is growing to further advancement as more vehicles are being produced primarily in Germany, Japan and the USA where japan has surpassed every other country with 92 refuelling stations. Toyota planned to produce 30,000 vehicles per year in 2020, Hyundai is targeting for 40,000 units per year production facility with 6.2 Billion US$ investment[2]. In 2019, it was forecasted that the fuel cells that were shipped for transport purposes would reach a capacity of almost 907.8 megawatts. The most fuel cell delivered to customers were from the transportation sector, and the supply has been increasing exponentially. This shows the potential of zero-emission- fuel cell application in the transportation section and interest of the business community but certain factors act as a barrier for possible commercialization. Fuel cell relies heavily on catalyst mainly platinum, a significant barrier to overcome cost-related issues in a fuel cell is platinum catalyst loading at cathode and anode. As per the breakdown analysis of cost, the catalyst costs around 41% of the total stack accounts for 500,000 units per year projected in 2017[3]. The projected cost for the fuel cell system is nearly around 45 USD/kW with a target of 30 USD per kW by the US Department of Energy. From the past decade, the commercial (FCV) sector focused on the reduction of platinum loading, which eventually reduces the total cost of the system. The platinum consumption in the commercial sector is widely varied for different numbers of applications. Auto-catalyst industries are significant sectors of platinum consumption in the market as much as 34.33%

as most of which is utilized in the fuel cell. Most of the platinum metal reserves available worldwide are present in South Africa, nearly 63,000 metric ton which is 95% of total reserves available today in Earth crust. Increasing demand and depleting reserves are one of the major concerns for fuel cell industrial applications. In 2017, the platinum loading targets had been reduced to 0.125 mg/cm^2 (around 10 g/vehicle) as compared to 1.0 mg/cm^2 (80g/vehicle) in 2002. Even the 10 g will add an additional cost of 300 USD per vehicle. Over time, there is a parallel relation in fuel cell system cost and catalyst loading, which results in a reduction of 84% system cost and 88% platinum loading[2]. In the past years, extensive research has been carried out for electrocatalyst for fuel cell, especially in PEMFC. The commercialization of PEMFC imposes constraints by limited power density and stability[4]. The catalyst must be able to bear extensive potential cycling and shutdown events for over 5000 hours lifetime and produce at least 1-1.5 A/cm^2 at 0.6 V_{RHE}. PEMFC faces several challenges with platinum as a catalyst due to corrosive conditions in the cell with very high overpotentials. Although, platinum is by the most active electrocatalyst for fuel cell, but the cost is the main factor. Another approach is to look for an alternative fuel cell that works on less corrosive environments with effective performance such as AEMFC and to look further on the development of non-PGM electrocatalysts. All of these will require an extensive amount of research to be done with numerous testing to benchmark new catalyst. Several methods are employed to benchmark electrocatalyst such as RDE, MEA, half cell GDE and floating electrode. The bottleneck for RDE technique is an unapproachable current density to real fuel cell conditions as the limiting current draws near to 6 mA/cm^2 at 1600 rpm at 0.9 V_{RHE}. RDE measurements are usually performed at ambient temperature and 1 bar oxygen partial pressure that limits the oxygen solubility in electrolyte hence resulting in low current densities due to low concentration and diffusion coefficients of dissolved gases. Fleige *et al.* improved the design of RDE by coupling magnetic drive to an electrochemical cell in the autoclave to enable high temperature (140°C) and pressure conditions (100 bars). These elevated conditions boosted the limiting current densities due to better solubility of reacting gases in liquid electrolyte[5]. Generally, the data from RDE is extrapolated to PEMFC relevant densities (0.6 V_{RHE} at 1.5–2.0 A/cm^2) usually approaches to significant errors. Catalyst performance can differ to a broad range from 0.6-0.9 V_{RHE} due to mass transport phenomena inside the catalyst layer. This could lead to misinterpretation of RDE results in which catalyst perform better at 0.9 V_{RHE} because the catalyst assembly is immersed in an electrolyte (oxygen saturated) providing superior access to electrons and protons while poor results for higher current densities in MEA. To overcome the gap and to take advantage of a fast and simplified method of RDE and high current densities of MEA, another method has been developed to benchmark catalyst in half cell gas diffusion electrode GDE setup for investigating the kinetics of electrocatalyst for ORR[6]. In this work, the PGM and non PGM electrocatalyst will be evaluated for ORR in novel GDE half-cell and the parameters affecting the catalyst will be observed to optimize the catalyst through influencing other parameters.

II. Experimental Methods

A. GDE Half Cell Measurements

To investigate the ORR activity of Fe-N-C catalyst, we operated the modified GDE half-cell developed by Ehelebe et al. [6] which was already used to benchmark platinum catalyst without any mass transport limitation and mimicked fuel cell conditions. The Figure **??** shows the schematic CAD view of GDE and cross-sectional view of electrode-electrolyte interface. The cell is made up of PTFE which has very high chemical resistance and strength[7]. The Viton O-rings were used for coupling the gas chamber to the electrolyte chamber. It provides better sealing due to high compressibility. The cell is comprised of two compartments, i.e. gas chamber and electrolyte compartment. The electrolyte compartment (holdup volume 250 ml) is comprised of two chambers, one for reference electrode and other for working electrode and electrolyte. The reference electrode compartment is connected to electrolyte compartment and working electrode interface by lugging capillary in a symmetrically oriented position (1mm apart from the electrode-electrolyte interface) to reduce ohmic resistance between the working and reference electrode (Ag/AgCl Metrohm). It does not impose any effect on electric field between working and counter electrode (expanded mesh of Ir/Ta mixed metal oxide [AN45272] on Ti, (METAKEM)). To limit the temperature variation up to 4 K, the distance between the counter and the working electrode is kept to minimum 1cm to depreciate cell resistance. The gas chamber comprised of low resistive (13 Ω m) graphite flow field (R8710, SGL CARBON) with channelling to ensure distributive gas flow over the gas diffusion electrode. The exposed area (2.01 cm^2) of gas diffusion electrode to the electrolyte is not compressed and supported by flow field from the back, which also serves as a current distributor. For unhindered conduction, the GDL is subjected to humidified gases (Air Liquide with purity 99.998% Ar, O_2 and synthetic air with 20% O_2 in N_2) in both electrolyte and gas compartment by commercial humidifier (Low Flow Humidification System, Fuel Cell Technologies, Inc) with mass flow controllers (EL-Flow Se- lect, Bronckhorst) at 3 bar. Biologic potentiostats (VSP-300) with two 2 A booster cable was used for data acquisition and parameters control (potential, current) for all experimental investigations of GDE half-cell.

1) Electrochemical Testing Protocol for GDE: Cyclic voltammetry measurements were being carried out in Ar saturated solution at 100 mV/s with the potential range of 0.05 to 1.2 V_{RHE} and reported with 100% correction (95% in-situ and 5% post-processing compensation). All the voltages were referenced to V_{RHE} which was measure before every experiment (around 0.015 to 0.026 V_{RHE} for $HClO_4$ and 1.015-1.026 V_{RHE} for KOH) with mesh counter electrodes and Ag-AgCl as a reference electrode. For ORR, spectroscopic galvanic impedance spectroscopy(SGEIS) technique has been carried out with O_2 flow (250 mln/min) from -0.1mA to -4A in both direction (forward and backward) within the range of 10

kHz to 10 Hz with 100% post-correction of iR compensation. The step was repeated until the achievement of reproducible results. After that, degradation cycles were carried out (5000-30000 cycles, depends on the requirement) within the potential limit of 0.6-1.0 V_{RHE} in saturated argon environment at a flow rate of 250 mln/min and SGEIS ORR was carried out again to see the stability of Fe-N-C after degradation cycles.

III. Results and Discussions

GDE method was chosen for this study to investigate the ORR phenomena, degradation and stability studies for the state of the art commercial platinum catalyst, advanced platinum catalyst (platinum nanoparticles on hollow graphite spheres) and non-platinum catalyst (Fe-N-C with different ionomers) in a mimicked fuel cell condition.

A. *Commercial Pt/C Catalyst*

1) Cleaning cycles impact: Before starting the ORR procedure, the catalyst was cleaned by cleaning cycles in the potential range of 0.05-1.2V_{RHE}. The appropriate cleaning cycles used for this study were 50, and it was already observed that prolonging the cleaning cycles may result in carbon corrosion[8]. To a certain extent, the carbon oxidation in our GDE cell is quite negligible due to our controlled parameters (scan rate 200 mV/s at room temperature), which is according to literature that carbon corrosion in insignificant until and unless fast scan rate at 500 mV/s is applied in the potential regime of 0.6-1.5 V_{RHE}[9]. The influence of impurities can be seen in CVs (Figure 1) by a distinctive difference between first and 50^{th} cleaning cycle.

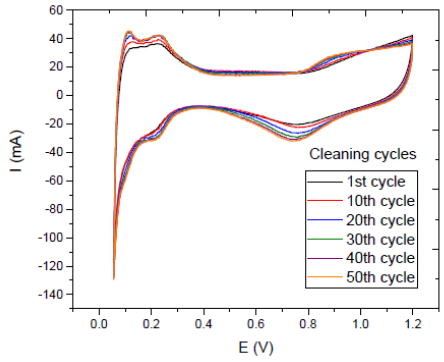

Fig. 1. Cleaning cycles for Pt/C HISPEC 4000 in GDE half-cell for PEMFC

In the first cycle, the peaks of oxidation are suppressed, and the current density is continuously increasing after cycles due to oxidation of organic impurities. In the high constant scan rate of 50-200 mV/sec, the process of impurities oxidation is faster, and the platinum surface is cleaned by adsorption of hydrogen and oxygen species and removal of organic impurities which is an important factor for further testing of catalyst. The attribute of potential cycling leads to real surface area exposure for better electrochemical reactions. However, there is a possibility of platinum dissolution over the range of 0.85 V_{RHE} as investigated by Cherevko *et al*[10].

2) Impact of non-membrane and membrane coated GDL catalyst layer on ECSA : All the commercial state of the art Pt/C catalysts were tested in the acid electrolyte with a concentration of 1.0 M $HClO_4$ and 1.0 M H_2SO_4 as shown in Figure 2. In the CVs, it can be seen that the oxidation current is higher for samples without a membrane (H_2SO_4 > $HClO_4$) with an onset voltage ≃0.8 V_{RHE} in the positive scan and this can be related to the formation of species (Oxygenated) on Pt such Pt-OH. In the negative scan, the reduction peaks are visible in the range of 0.6-0.8 V_{RHE} leading to reduction of Pt oxides. The onset voltage of Pt catalyst in H_2SO_4 for the formation of oxygenated species shifted the peak current mainly caused by anion adsorption with a difference of 0.8V_{RHE} for $HClO_4$ to 0.85 V_{RHE} for H_2SO_4 through strong bisulfate adsorption. Although the CVs were determined in an oxygen-free environment, the presence of O_2 in the electrolyte is visible in the down bulge peaks at around 0.75 V_{RHE} affecting the redox reaction of Pt/C where the reduction occurs. The samples without membranes were least affected by the reduction, and there is a significant increase in reduction currents for GDL without membranes. After integrating the H_{UPD} regions, the electrochemical surface area of Pt/C electrocatalyst is found to be as 66.59 m^2/g_{pt} in $HClO_4$, 61.55 m^2/g_{pt} in H_2SO_4, 53.67 m^2/g_{pt} in $HClO_4$(with membrane) and 25.49 m^2/g_{pt} in H_2SO_4 (with membrane). The sequential order in ECSA is similar to the CVs, but it was also observed that some factors could be subjected to uneven estimation of ECSA.

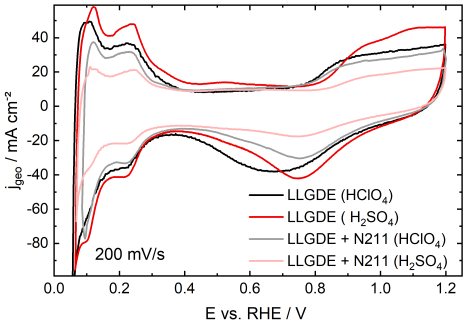

Fig. 2. Comparison fo CVs for commercial Pt/C catalyst with 0.3mg_{Pt}/cm^2 in $HClO_4$ and H_2SO_4 with and without membranes

3) ORR performance in O_2 and Synthetic air (SA) purged cathode in $HClO_4$ and H_2SO_4 : The polarization curve and Tafel plot during ORR was first determined in oxygen via SGEIS technique with forwarding and backward scans showing the typical redox behaviour of electrocatalyst in O_2 and synthetic air in Figure 3. The samples were tested with and without membrane in both $HClO_4$ and H_2SO_4 and compared the activity with previous literature to analyze the effect of the bonded membrane to ORR activity.

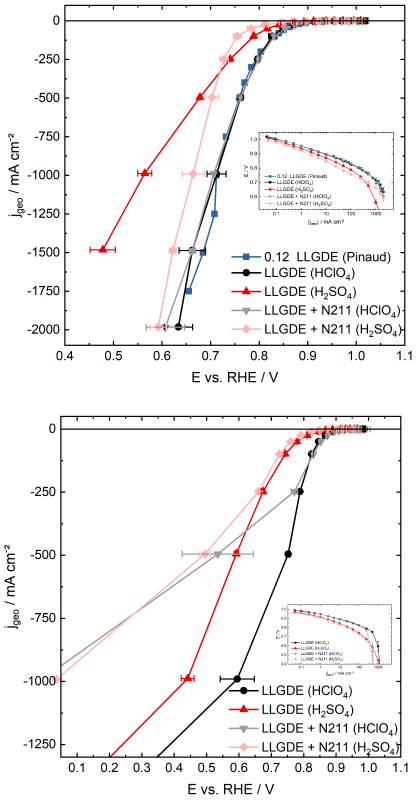

Fig. 3. Polarization curve of commercial Pt/C for ORR in O_2 and SA obtained via SGEIS

In Figure 3, it is revealed that the Pt/C in $HClO_4$ approached to high limiting current density of 2 A/cm^2 from 0.607-0.633 V_{RHE}. At 0.66 V_{RHE} and 1.5 A/cm^2, both polarization curves of Pt/C with and without membrane were similar, but then the divergence appears with a difference of $\simeq$ 26 mV. Although, both samples exhibited the same onset and half-wave potential onset (E_{onset} 0.871 V_{RHE}, $E_{1/2}$ 0.706 V_{RHE}). This difference can be regarded as flooding at the catalyst surface, which can be minimized with additional cycling. In comparison to other GDE study, the results agree with other researchers[6], [11].

4) Activity of commercial Pt /C catalyst in alkaline media for AEMFC in GDE half-cell setup: Due to corrosive nature of acidic electrolyte, the alkaline and neutral electrolytes research has been increased in past years. Alkaline electrolyte grabbed major attention due to beneficial properties of stable environment while imposing the problems of membranes stability. The CVs of platinum in alkaline gives different features as compared to CVs in acid, especially in H*upd* region, the peaks of hydrogen adsorption occupy the different onset potential approaching to a contracted double layer region. In the underpotential deposition regions, the peaks between 0.25-0.4 V_{RHE} attributed to the interactive sites of Pt(110) and Pt(100) and this is a crucial region due to anions adsorption on the surface from electrolyte. The position of peaks for their relative surface plane is similar to the single crystal Pt in alkaline media and due to the minor shift after ORR towards more positive onset, it can be assumed some inhabitation effect occurred by blocked sites[12], [13].

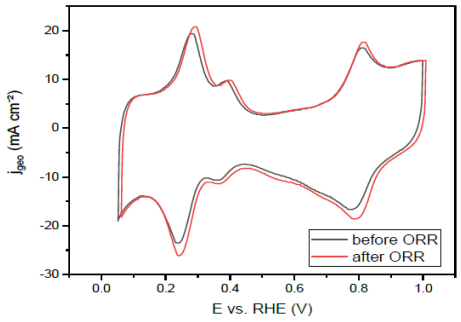

Fig. 4. CVs of Pt/C HISPEC 4000 in 1.0M KOH

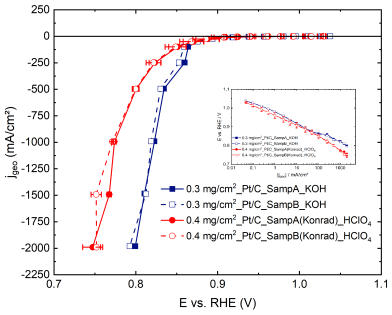

Fig. 5. Polarization Tafel plot of Pt/C HISPEC 4000 in 1.0M KOH

By integrating the H*upd*, the determined ECSA was found to be 72 m^2/g$_{pt}$ which is slightly higher than the available surface area in literature i.e. 62 m^2/g$_{pt}$. The ORR conducted in $HClO_4$ and KOH with similar catalyst can be seen in Figure 7 and there is a significant comparison. Although, it is well known that ORR in acid electrolyte for Pt/C catalyst with relatively high performance in PEMFC but ORR in alkaline electrolyte for Pt/C in AEMFC is still yet to explore. Due to versatility of GDE, the commercial Pt/C HISPEC-4000 was investigated at high current densities. The catalyst in KOH exhibited very high activity of approaching to 2 A/cm^2 at 0.799V_{RHE} with a high onset value of 0.88 V_{RHE}. In alkaline solution, the reaction needed less activation energy approaching to high current density. While approaching to 2 A/cm^2, the activity was changing linearly with a different of 10-20 mV from 500-2000 mA/cm^2. The same behaviour was observed in second sample, therefore, the reproducibility of GDE for this experiment can be observed. In comparison to ORR in $HClO_4$, the catalyst exhibited lower activity to alkaline approach it 2 A/cm^2 at 0.751 V_{RHE} with almost the similar onset and the results in $HClO_4$ agree with previous literature. The difference in activities for ORR started at high current densities from 100 mA/cm^2 up to 2A/cm^2 with an increasing difference of 20-40 mV. Even though, the activity of Pt/C in alkaline is relatively high then latest research

approaching to 0.73 V_{RHE} at 2A/cm^2, the results in GDE are not conclusive.

B. *Advanced Pt/HGS Catalyst*

1) Impact of stress cycling on the activity enhancement of Pt/HGS: In this work, the effects of break in procedure and AST cycles were carried out in a GDE half-cell to investigate the highest possible activity of Pt/HGS in 1.0 M $HClO_4$. The approach is to get a state to achieve maximum activation through intense cycling by applying positive potential from 0.4-1.0 V_{RHE}. The cycling can help to detach the carbon layer over the active sites of sintered Pt nanoparticles and helps in providing the better accessibility for reaction. In the lab investigations done previously (not published), it has been found that Pt/HGS requires aging (10,000 cycles) to reach it maximum potential activity and it will show better performance in PEMFC due to high oxygen diffusion through mesoporous structure.

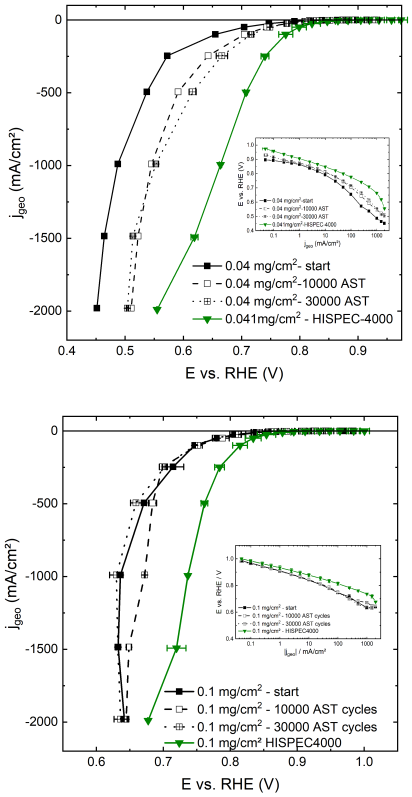

Fig. 6. Polarization curve and Tafel plot showing ORR performance changes with stress cycling in 1M $HClO_4$ for low loading Pt/HGS

In order to understand the effect of aging and the catalyst loading impact on the ORR performance, samples with loading 0.04mg_{Pt}/cm^2 and 0.1 mg_{Pt}/cm^2 were prepared and the test has been done twice to check the reproducibility of results. The impact of loading of state-of-the-art Pt/C has been extensively studied by various researchers that showed that the ORR performance is also dependent on optimal catalyst loading. It can be seen in polarization curve Figure 6 that sample with higher loading of 0.1 mg_{Pt}/cm^2 approached the limited current density of 2 A/cm^2 at 0.65 V_{RHE} with almost the same half wave potential and onset potential of 0.75 V_{RHE}. The second sample of same loading exhibited the exactly similar trend. The sample with low loading of 0.04 mg_{Pt}/cm^2 approached the limited current density of $\simeq$0.45 V_{RHE} (average) at the limiting current density of 2 A/cm^2. The onset potential of this sample was very low compared to higher loading sample with E_{onset} $\simeq$0.6 V_{RHE}, therefore, low loading sample exhibited the higher activation losses. The difference of activities in both samples is less at low current densities while it is broadening as the polarization approaches to limiting current density with a difference of $\simeq$20 mV, the trend is also similar to the catalyst investigation for Pt/C catalyst in GDE half-cell. The OCV of higher and lower Pt loading ranges from $\simeq$0.9-1.0 V_{RHE}.

2) ECSA determination and complications for Pt/HGS: The impact of activation can be seen during the intensive AST cycles effecting the surface area which ultimately have an impact on catalyst utilization. In order to verify the statement from Pt/HGS manufacturers that the catalyst will achieve the maximum activity after subjecting to 10000 AST cycles, the catalyst in this research was subject to 30,000 AST cycles as standardized by DOE to see after effects of 10K cycles. The activation cycles can increase the electrochemically active surface area. In the beginning, before and after ORR cycling, the ECSA was found to be $\simeq$50.84-52 m^2/g$_{pt}$ which increased after 2500 cycles to 62 mm^2/g$_{pt}$ and then remain stable till 10k cycles with ECSA of 60 m^2/g$_{pt}$. Eventually after 30,000 cycles, the ECSA reduced to lowest as 44.08 m^2/g$_{pt}$ by not be able to retain its initial surface area. Although, it is challenging to subject catalyst to cyclic voltammetry cycles continuously which requires stable cathode catalyst design to give reproducible results which is still challenging in fuel cell but can be achieved by well controlled conditions[14]. Initially, the ECSA was similar showing that the catalyst is not subjected to particles agglomeration and growth, the chances of carbon corrosion is also negligible due to ECSA increases from 2500-10K cycles.

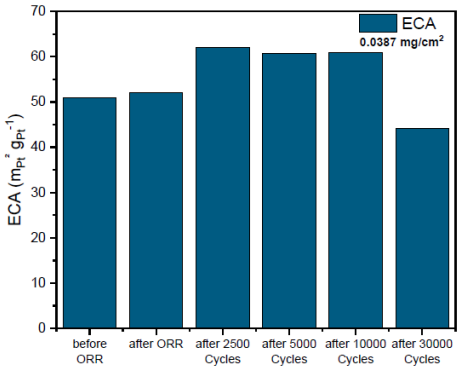

Fig. 7. ECSA variation during stress cycling in 1.0 M $HClO_4$ for Pt/HGS

C. *Non PGM Fe-N-C Catalyst*

1) Degradation in AST Oxygen (O_2) and Argon (Ar): The degradation of Fe-N-C influenced by Oxygen is well understood for PEMFC due to production of Fenton reagent and has been studied before but there is still a gap for degradation mechanism in AEMFC for Fe-N-C which is addressed in this work. The impact of gases (O_2 and Ar) can impose different performance degradation behaviour during the stress cycling. The Fe-N-C catalyst was examined for degradation through AST by cycling continuously in the potential range of 0.6-1.2 V_{RHE} in Ar and O_2 for 5000 degradation cycles. Under certain specific conditions, the catalyst was subject to degradation by accelerating the cycles to 100 mV/sec leading to faster redox reaction. Figure 8 represents the polarization curve and Tafel plot, the ORR measurement has been carried out in a period of time before and after AST, in comparison to limited current density of 2A/cm^2, the samples with Ar purged AST showed better performance after AST with an increase in ORR activity from 0.49 V_{RHE} to 0.509 V_{RHE}.

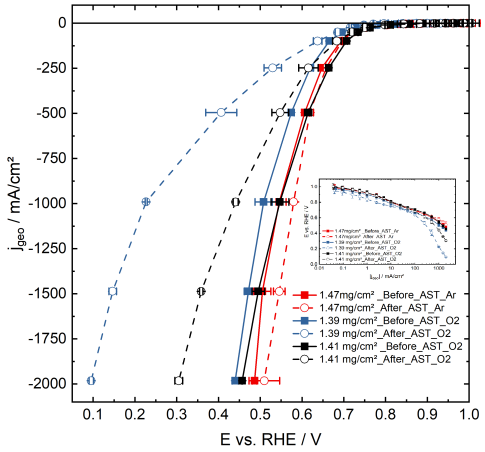

Fig. 8. Polarization curve of Fe-N-C with average loading 1.5 mg_{Fe-N-C}/cm^2 facing degradation during ORR in $O_2$and Ar

The better activity after ORR gives a clue that activation of sample can be required before experiment. However, the severe degradation of catalytic activity occurred for AST with O_2 from 0.49-0.233 V_{RHE}. It is interesting that catalyst was stable and showed similar ORR activity at high current density region to that of Ar-AST samples.

2) Impact of Ion Exchange Capacity IEC: The Fe-N-C catalyst coated GDL was prepared with commercial Fe-N-C Pajarito powder and commercial ionomer Aemion^{TM}, both are optimized for utilization in AEMFC to operate without the use of PGM. The ionomer is classified into two categories with different ion exchange capacities (IEC) *i.e.* high ion exchange capacity ionomer (HIEC) and low ion exchange capacity ionomer (LIEC). In this section, the comparison and behaviour of Fe-N-C with different IEC is investigated. The main issue that affects the AEMFC performance is the degradation (chemical) of ion exchange material either ionomer or anion exchange membrane, which makes it unable to achieve the high activity as compared to Pt and its alloys in PEMFC. This degradation effect is caused by nucleophilic attack and some elementary reactions between OH^- anions and functional groups of ion exchange material[15]. Due to instability issue, the purpose of this work is to optimize the ionomer for better stability regardless of high performing activity. Despite of the efforts made for optimizing and synthesizing the novel functional group, the high current density and stability is yet to achieve[16]. The polarization curve of samples HIEC and LIEC with loading $\simeq 1.73 V_{RHE}$ is shown in Figure 9.

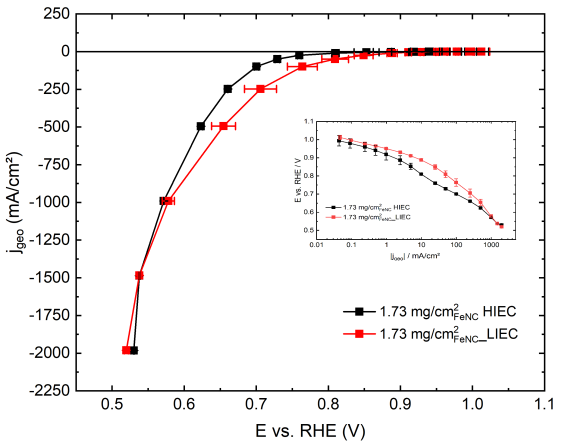

Fig. 9. Polarization curve showing the performance difference for high and low anion exchange capacity ionomer

Both sample exhibited almost similar activity in O_2 ORR such as HIEC achieved 0.53 V_{RHE} at limiting current density of 2A/cm^2 and LIEC with 0.51 V_{RHE} at 2 A/cm^2 . The activation required for both samples are different as HIEC with onset of 0.8 V_{RHE} and LIEC with onset of 0.88 V_{RHE} showing that high activation needed for sample with high IEC. Interesting, as approaching to half wave potential, the performance of LIEC was better but the error bar shows that there is a difference in between forward and backward scan showing that LIEC suffers from water imbalance issue. After achieving the half wave potential, the HIEC performance enhanced surpassing the LIEC activity at limiting current density showing that IEC content can impact the performance and stability at high current density. In the Tafel plot (figure 9, the OCV of LIEC and HIEC Fe-N-C was found to be 0.99-1.01 V_{RHE} which is below thermodynamic value of H_2/O_2 fuel cell showing the activation losses. The LIEC Tafel slope of 51 mV/dec was achieved in the low current density region of 0.1-10 mA/cm^2 from 0.8-1.0 V_{RHE} and 181.94 mV/dec in the high current density region. This transition of high slope of Tafel plot shows that catalyst was subjected to degradation from 0.8 V_{RHE} which is high above the fuel cell limiting degradation potential of 0.6 V_{RHE}. The HIEC

Tafel slope of 99.89 mV/dec was achieved in low current density region of 0.1-10 mA/cm^2 from 0.7-0.95 V_{RHE} and 102.11 mV/dec in the high current density regions which shows that the performance degradation in the high current region for HIEC is not much bad as for LIEC. Regarding IEC of ionomers, Aemion^{TM} activity with higher efficiency and OH- conductivity is significantly better as compared to other ionomers with high IEC 1.3 meq/g[17]. The high IEC leads to high ionic conductivity, more water uptake which results in more dimensional swelling.

3) Catalyst layer optimization of Fe-N-C LIEC by Activation Procedure: The Fe-N-C catalyst coated GDL layers prepared by doctor blading were in the range of 1.5-1.7 mg/cm^2 and shown as an average in results which were immersed in KOH to achieve high conductivity[18]. Several break in procedures were carried out in Ar saturated environment during cyclic voltammetry to initiate the activation. The polarization curve and Tafel plot of all samples (averaged) in linear and logarithmic scale is demonstrated, the 48h sample exhibit the high onset and have less linear drop during activation losses, however the sample with 72h loading have rapid drop during activation losses and with much severe mass transport limitation as compared to other activation time. In comparison to activation losses, the sample with 48h activation exhibits the onset at 0.8 V_{RHE} (Figure 10), the activity of all samples reduced gradually in the kinetic controlled region (0.6-0.9 V_{RHE}).

In the Tafel plot (Figure10), 48h activation exhibited high performance while the 72h activation fall below the non-activated samples. Variation in the activity is due to loss of cationic active sites, ion dilution and swelling along with long term immersion of CCM in electrolyte that increases the impurity ions which needed to be removed accordingly[18], [19]. The 72h immersion showed significant low performance, the would be possible due to two reason, Fe-N-C catalyst or ionomer stability (resulting due to OH- attack at the C2 position of Benzimidazolium ring)[20]. Another possibility for less activity in the high current density region is due dimensional swelling and water uptake for monovalent anion as reported in literature that OH^- ions can lead to more dimensional swelling as compared to CL^- and I^- ions[19], [21]. In the Kinetic region (around 0.8 V_{RHE}), all the samples exhibited the similar performance.

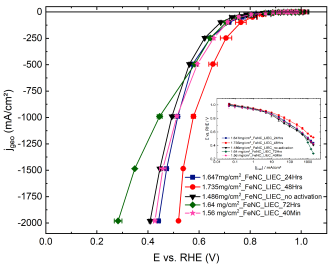

Fig. 10. Fe-N-C LIEC Polarization curve showing the catalyst layer optimization by activation time

4) Reproducibility Fe-N-C HIEC: To investigate the reproducibility of results, Fe-N-C HIEC GDLs were prepared with loading from 0.89-1.73 mg/cm^2 for ORR in O_2.

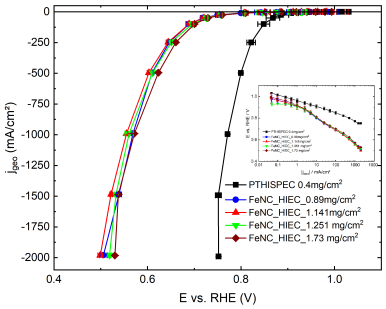

Fig. 11. Fe-N-C HIEC Polarization curve showing the reproducibility of results

The polarization curve in Figure 11 depicts the performance of Fe-N-C in comparison to commercial Pt/C to the limiting current density of 2 A/cm^2 The impact of loading can be seen that as the catalyst loading increases, the activity gets better but to a certain extent. The Fe-N-C achieved the limiting current density of 0.49-0.53 V_{RHE} at 2 A/cm^2 with higher onset of 0.80 V_{RHE} which agrees with our previous results. Unlike Pt/C which very high activity of 0.7 V_{RHE} at 2A/cm^2 in acid electrolyte, the Fe-N-C perceived very high activation losses which is subjected to hydration level of anion exchange material. Despite the similar performance in polarization curve, all samples have different OCV without correlation to loading and the activity degradation starts at 0.8 V_{RHE} in the low current density region with increasing slope in high current density region (Figure 11). The performance gap is huge between Pt/C and Fe-N-C HIEC which may require some more activation study to optimize the catalyst layer properties.

5) Stability of Fe-N-C with HIEC Ionomer in ORR O_2: To address the stability of catalyst and ionomer in alkaline, the optimized Fe-N-C with anion conducting ionomer HIEC is subjected to ORR in O_2 before and after 5000 AST degradation cycles in Ar. With the use of high conductive ionomer Aemion^{TM} HIEC, the Fe-N-C was able to achieve and maintain its performance at high current density. The

performance of Fe-N-C is similar after subjecting to 5000 degradation cycles with onset of 0.801 V_{RHE} and approached limiting current density of 2 A/cm^2 at 0.53 V_{RHE}. Similarly, the OCV value for measurements is similar $\simeq$1.0 V_{RHE} with a Tafel slope of 110.2 mV/dec in low current density region of 0.1 mA/cm^2 to 10 mA/cm^2 from 0.8-1.0 V_{RHE}. As approaching to high current density, the cathode is subjected to water starvation which leads to severe hydration of anion exchange material and thus the catalyst will be acquiring a high activation energy and overpotentials, which can be seen in the polarization curve.

6) Impact of non-Optimized Fe-N-C with H^+ Conducting Ionomer Nafion^{TM}: The Fe-N-C in acid electrolyte has been studied in past years but it still hasn't gained much attention due to low initial activity for ORR[22]–[24]. To see the effect of type of ionomer, Nafion^{TM}is added to Fe-N-C Pajarito Powder and the effect can be seen in polarization curve Figure 12.

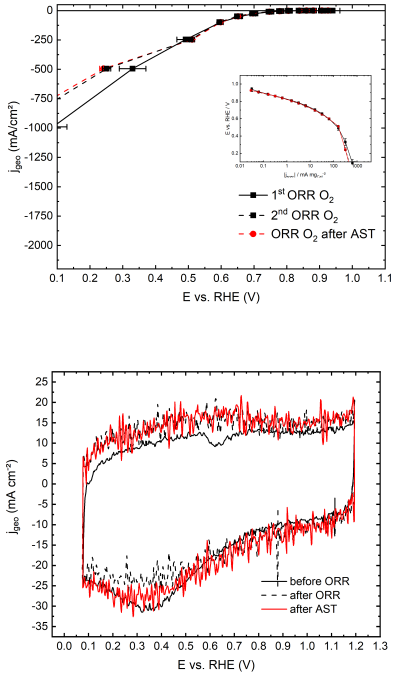

Fig. 12. Severe degradation of Fe-N-C with proton conducting ionomer in Acid electrolyte

The catalyst was subjected to sequential ORR in O_2 to investigate any effect on the performance. The activity of catalyst degrades gradually with less positive onset and approach to mass transport limitation without reaching to the limiting current density of GDE *i.e.* 2 A/cm^2. In the first ORR measurement, the Fe-N-C approached to 930 mA/cm^2 at 0.1 V_{RHE} which reduced to 750 mA/cm at 0.1 V_{RHE} for second and third (after 5000 degradation cycles) ORR measurement. Now, if we look in CVs Figure 12, the voltammogram is not stable with fluctuation in current density in both scans and the pseudo capacitance is changing with increasing potential. The disturbance in the system yet not enabled GDE to investigate the catalyst layer properties as the problem is continuous since we have got reproducible results for this experiment. Now taking consideration of Fe-N-C and Nafion^{TM}, the catalyst is optimized for AEMFC alkaline solution especially KOH electrolyte. The Nafion is mostly used for PGM catalyst as binder in PEMFC while the iron is most subjected to corrosion and dissolution in acid. Although, Fe-N-C showed a suitable activity for ORR in acid, but its combination with different electrocatalyst is a broad field of research. Now taking consideration of Fe-N-C and Nafion^{TM},the catalyst is not optimized for PEMFC. The Nafion is mostly used for PGM catalyst as binder in PEMFC which shows that the problem doesn't occurred due to ionomer. More investigation will be required by extensive series of experiment with additional surface characterization. However, there is not much research available for the proper understanding of the combination of Fe-N-C with Nafion degradation on a molecular level and there is still a gap to identify the root cause of the problem either the problem lies in the conduction of ionomer or the water management issue causes the observable performance degradation.

IV. Conclusions

In this research, all research objectives were met to analyze the versatility of GDE half cell investigation. The electrolyte and membrane can affect the performance of ORR electrocatalyst as observed in the commercial Pt/C with and without membrane in different acid electrolyte ($HClO_4$ and H_2SO_4). The radical chlorine and sulfate ions can poison the catalyst active and the probability of Pt dissolution is high due to uncertain events of amplifier overloading. It has been found that diprotic effect of H_2SO_4 can limit the activity of commercial Pt/C and the higher affinity to sulfate ions on catalyst layer can reduce the performance and subjected to high mass transport limitation and it can be overcome with introduction of ion conducting Nafion membrane. The Pt/C HISPEC 4000 with loading 0.3 mg/cm^2 approached to limiting current density of 2 A/cm^2 at 0.63 V$_{RHE}$ in 1.0 M $HClO_4$, the catalyst showed very high performance in KOH in contrast to the literature which shows the overestimation of performance and it is considered as a drawback in GDE half cell measurements. The advanced Pt/HGS was evaluated in 1.0M $HClO_4$ to investigate the results from the scientists that it can reach to maximum activity after subjecting to 10k degradation cycles. Finally, the GDE half-cell was conditioned to mimic the AFC for optimization of non PGM electrocatalyst Fe-N-C (Pajarito powder) and high anion conducting ionomer Aemion^{TM} with different ion exchange capacity. The catalyst layer was optimized by immersing the catalyst coated GDL in 1.0 M KOH for 48 hours demonstrating the best performance and the catalyst showed very high and uniform stability with 5000 AST cycles in the potential sweep of 0.6-1.0 V$_{RHE}$. Several other investigations can be done in GDE such as ECSA determination by CO stripping to tackle the issues we faced during H_2 stripping and investigation of Pt-alloys for ORR in the half cell. Due to quick and fast track GDE methods, it

is possible to quickly investigate numerous catalysts in short period of time but this investigation sometimes doesn't tell the full story such as catalyst morphological changes during cycling, the amount of catalyst dissolution, these properties can be accommodated by combining GDE with other tools such as TEM and scanning flow cell for future work.

Acknowledgment

I would like to acknowledge Helmholtz Institute Erlangen-Nürnberg (HI ERN), Forschungszentrum Jülich, Insitiuto Superior Tecnico Lisbon, AGH University of Science and Technology, EIT Innoenergy for sponsoring my work. This thesis work is shared for double degree program MSc Energy Transition to IST Portugal and AGH UST Poland.

References

[1] European Environmental Agency, "Greenhouse gas emissions from transport in Europe," Tech. Rep., 2019, IND–111. [Online]. Available: https://www.eea.europa.eu/data-and-maps/indicators/transport-emissions-of-greenhouse-gases/transport-emissions-of-greenhouse-gases-12.

[2] B. Pivovar, "Catalysts for fuel cell transportation and hydrogen related uses," *Nature Catalysis*, vol. 2, no. 7, pp. 562–565, Jul. 2019, ISSN: 2520-1158. DOI: 10.1038/s41929-019-0320-9. [Online]. Available: http://www.nature.com/articles/s41929-019-0320-9.

[3] J. Marcinkoski, J. Spendelow, A. Wilson, and D. Papageorgopoulos, "DOE Hydrogen and Fuel Cells Program Record - Fuel Cell System Cost - 2017," *Journal of Mechanisms and Robotics*, vol. 9, no. 4, pp. 1–9, 2017, ISSN: 1942-4302. DOI: 10.1115/1.4036738. [Online]. Available: http://mechanismsrobotics.asmedigitalcollection.asme.org/article.aspx?doi=10.1115/1.4036738.

[4] X. X. Wang, M. T. Swihart, and G. Wu, "Achievements, challenges and perspectives on cathode catalysts in proton exchange membrane fuel cells for transportation," *Nature Catalysis*, vol. 2, no. 7, pp. 578–589, 2019, ISSN: 2520-1158. DOI: 10.1038/s41929-019-0304-9. [Online]. Available: http://dx.doi.org/10.1038/s41929-019-0304-9.

[5] M. J. Fleige, G. K. H. Wiberg, and M. Arenz, "Rotating disk electrode system for elevated pressures and temperatures," *Review of Scientific Instruments*, vol. 86, no. 6, p. 064 101, Jun. 2015, ISSN: 0034-6748. DOI: 10.1063/1.4922382. [Online]. Available: http://aip.scitation.org/doi/10.1063/1.4922382.

[6] K. Ehelebe, D. Seeberger, M. T. Y. Paul, S. Thiele, K. J. J. Mayrhofer, and S. Cherevko, "Evaluating Electrocatalysts at Relevant Currents in a Half-Cell: The Impact of Pt Loading on Oxygen Reduction Reaction," *Journal of The Electrochemical Society*, vol. 166, no. 16, F1259–F1268, Nov. 2019, ISSN: 0013-4651. DOI: 10.1149/2.0911915jes. [Online]. Available: https://iopscience.iop.org/article/10.1149/2.0911915jes.

[7] S. V. Gangal and P. D. Brothers, "Perfluorinated Polymers, Polytetrafluoroethylene," in *Encyclopedia of Polymer Science and Technology*, Wiley, Jun. 2010. DOI: 10.1002/0471440264.pst233.pub2. [Online]. Available: https://onlinelibrary.wiley.com/doi/abs/10.1002/0471440264.pst233.pub2.

[8] I. Savych, S. Subianto, Y. Nabil, S. Cavaliere, D. Jones, and J. Rozière, "Negligible degradation upon in situ voltage cycling of a PEMFC using an electrospun niobium-doped tin oxide supported Pt cathode," *Physical Chemistry Chemical Physics*, vol. 17, no. 26, pp. 16 970–16 976, 2015, ISSN: 1463-9076. DOI: 10.1039/C5CP01542A. [Online]. Available: http://xlink.rsc.org/?DOI=C5CP01542A.

[9] E. Pizzutilo, S. Geiger, J.-P. Grote, A. Mingers, K. J. J. Mayrhofer, M. Arenz, and S. Cherevko, "On the Need of Improved Accelerated Degradation Protocols (ADPs): Examination of Platinum Dissolution and Carbon Corrosion in Half-Cell Tests," *Journal of The Electrochemical Society*, vol. 163, no. 14, F1510–F1514, 2016, ISSN: 0013-4651. DOI: 10.1149/2.0731614jes. [Online]. Available: https://iopscience.iop.org/article/10.1149/2.0731614jes.

[10] S. Cherevko, G. P. Keeley, S. Geiger, A. R. Zeradjanin, N. Hodnik, N. Kulyk, and K. J. J. Mayrhofer, "Dissolution of Platinum in the Operational Range of Fuel Cells," *ChemElectroChem*, vol. 2, no. 10, pp. 1471–1478, Oct. 2015, ISSN: 21960216. DOI: 10.1002/celc.201500098. [Online]. Available: http://doi.wiley.com/10.1002/celc.201500098.

[11] B. A. Pinaud, A. Bonakdarpour, L. Daniel, J. Sharman, and D. P. Wilkinson, "Key Considerations for High Current Fuel Cell Catalyst Testing in an Electrochemical Half-Cell," *Journal of The Electrochemical Society*, vol. 164, no. 4, F321–F327, Feb. 2017, ISSN: 0013-4651. DOI: 10.1149/2.0891704jes. [Online]. Available: https://iopscience.iop.org/article/10.1149/2.0891704jes.

[12] T. J. Schmidt, V. Stamenkovic, P. N. Ross, Jr., and N. M. Markovic, "Temperature dependent surface electrochemistry on Pt single crystals in alkaline electrolyte," *Physical Chemistry Chemical Physics*, vol. 5, no. 2, pp. 400–406, Jan. 2003, ISSN: 14639076. DOI: 10.1039/b208322a. [Online]. Available: http://xlink.rsc.org/?DOI=b208322a.

[13] N. M. Markovića, S. T. Sarraf, H. A. Gasteiger, and P. N. Ross, "Hydrogen electrochemistry on platinum low-index single-crystal surfaces in alkaline solution," *J. Chem. Soc., Faraday Trans.*, vol. 92, no. 20, pp. 3719–3725, 1996, ISSN: 0956-5000. DOI: 10.1039/FT9969203719. [Online]. Available: http://xlink.rsc.org/?DOI=FT9969203719.

[14] J. Durst, A. Lamibrac, F. Charlot, J. Dillet, L. F. Castanheira, G. Maranzana, L. Dubau, F. Maillard, M. Chatenet, and O. Lottin, "Degradation heterogeneities induced by repetitive start/stop events in proton exchange membrane fuel cell: Inlet vs. outlet and channel vs. land," *Applied Catalysis B: Environmental*, vol. 138-139, pp. 416–426, Jul. 2013, ISSN: 09263373. DOI:

10 . 1016 / j . apcatb . 2013 . 03 . 021. [Online]. Available: https : / / linkinghub . elsevier . com / retrieve / pii / S092633731300180X.

[15] S. Gottesfeld, D. R. Dekel, M. Page, C. Bae, Y. Yan, P. Zelenay, and Y. S. Kim, "Anion exchange membrane fuel cells: Current status and remaining challenges," *Journal of Power Sources*, vol. 375, pp. 170–184, Jan. 2018, ISSN: 03787753. DOI: 10.1016/j.jpowsour.2017.08.010. [Online]. Available: https://linkinghub.elsevier.com/retrieve/pii/S0378775317310340.

[16] D. R. Dekel, "Review of cell performance in anion exchange membrane fuel cells," *Journal of Power Sources*, 2018, ISSN: 03787753. DOI: 10.1016/j.jpowsour.2017.07.117.

[17] L. Sun, J. Guo, J. Zhou, Q. Xu, D. Chu, and R. Chen, "Novel nanostructured high-performance anion exchange ionomers for anion exchange membrane fuel cells," *Journal of Power Sources*, vol. 202, pp. 70–77, Mar. 2012, ISSN: 03787753. DOI: 10.1016/j.jpowsour.2011.11.023. [Online]. Available: https://linkinghub.elsevier.com/retrieve/pii/S0378775311022142.

[18] N. Ziv and D. R. Dekel, "A practical method for measuring the true hydroxide conductivity of anion exchange membranes," *Electrochemistry Communications*, vol. 88, pp. 109–113, Mar. 2018, ISSN: 13882481. DOI: 10 . 1016 / j . elecom . 2018 . 01 . 021. [Online]. Available: https://linkinghub.elsevier.com/retrieve/pii/S1388248118300286.

[19] C. G. Arges and L. Zhang, "Anion Exchange Membranes' Evolution toward High Hydroxide Ion Conductivity and Alkaline Resiliency," *ACS Applied Energy Materials*, vol. 1, no. 7, pp. 2991–3012, Jul. 2018, ISSN: 2574-0962. DOI: 10.1021/acsaem.8b00387. [Online]. Available: https://pubs.acs.org/doi/10.1021/acsaem.8b00387.

[20] O. D. Thomas, K. J. Soo, T. J. Peckham, M. P. Kulkarni, and S. Holdcroft, "A stable hydroxide-conducting polymer," *Journal of the American Chemical Society*, 2012, ISSN: 00027863. DOI: 10.1021/ja303067t.

[21] A. G. Wright, J. Fan, B. Britton, T. Weissbach, H.-F. Lee, E. A. Kitching, T. J. Peckham, and S. Holdcroft, "Hexamethyl-p-terphenyl poly(benzimidazolium): a universal hydroxide-conducting polymer for energy conversion devices," *Energy & Environmental Science*, vol. 9, no. 6, pp. 2130–2142, 2016, ISSN: 1754-5692. DOI: 10.1039/C6EE00656F. [Online]. Available: http://xlink.rsc.org/?DOI=C6EE00656F.

[22] F. Jaouen, V. Goellner, M. Lefèvre, J. Herranz, E. Proietti, and J. P. Dodelet, "Oxygen reduction activities compared in rotating-disk electrode and proton exchange membrane fuel cells for highly active FeNC catalysts," *Electrochimica Acta*, vol. 87, pp. 619–628, 2013, ISSN: 00134686. DOI: 10.1016/j.electacta.2012.09.057. [Online]. Available: http://dx.doi.org/10.1016/j.electacta.2012.09.057.

[23] D. Singh, K. Mamtani, C. R. Bruening, J. T. Miller, and U. S. Ozkan, "Use of H2S to probe the active sites in FeNC catalysts for the oxygen reduction reaction (ORR) in acidic media," *ACS Catalysis*, vol. 4, no. 10, pp. 3454–3462, 2014, ISSN: 21555435. DOI: 10.1021/cs500612k.

[24] K. Mamtani, D. Singh, J. Tian, J. M. M. Millet, J. T. Miller, A. C. Co, and U. S. Ozkan, "Evolution of N-Coordinated Ironâ"Carbon (FeNC) Catalysts and Their Oxygen Reduction (ORR) Performance in Acidic Media at Various Stages of Catalyst Synthesis: An Attempt at Benchmarking," *Catalysis Letters*, 2016, ISSN: 1572879X. DOI: 10.1007/s10562-016-1800-z.